Geodesy and Geodynamics 8 (2017) 221–228

Contents lists available at ScienceDirect

Geodesy and Geodynamics

journal homepages: www.keaipublishing.com/en/journals/geog; http://www.jgg09.com/jweb_ddcl_en/EN/volumn/home.shtml

Ionospheric disturbances associated with the 2015 *M*7.8 Nepal earthquake

Yiyan Zhou [a, b, *], Jian Yang [a, b], Fuying Zhu [a, b], Fanfan Su [a, b], Liangchen Hu [a, b], Wenbo Zhai [a, b]

[a] *Institute of Seismology, China Earthquake Administration, Wuhan, 430071, China*
[b] *Key Laboratory of Earthquake Geodesy, China Earthquake Administration, Wuhan, 430071, China*

ARTICLE INFO

Article history:
Received 8 December 2016
Accepted 20 April 2017
Available online 8 May 2017

Keywords:
GPS
TEC
*M*7.8 Nepal earthquake
Pre-earthquake ionospheric anomalies
CID

ABSTRACT

Based on the total electron content (TEC) derived from Global Positioning System (GPS) observations of the Crustal Movement Observation Network of China (CMONOC) and the Global Ionosphere Map (GIM) from the Center for Orbit Determination in Europe (CODE), we detected and analyzed the ionospheric variations during the 2015 *M*7.8 Nepal earthquake (including the pre-earthquake ionospheric anomalies and coseismic ionospheric disturbances (CIDs) following the main shock). The analysis of vertical total electron content (VTEC) time series shows that the large-scale ionospheric anomalies appeared near the epicenter two days prior to the earthquake. Moreover, the pre-earthquake ionospheric anomalies were also observed in the geomagnetically conjugated region. In view of solar-terrestrial environment, the pre-earthquake ionospheric anomalies could be associated with the Nepal earthquake. In addition, we also detected the CIDs through the high-frequency GPS observation stations. The CIDs had obvious oscillated waveforms with the peak-to-peak disturbance amplitudes of about 1 TECu and 0.4 TECu, which propagated approximately with the horizontal velocities of 877 ± 75 m/s and 319 ± 30 m/s, respectively. The former is triggered directly by the acoustic waves which originated from the energy release of the earthquake near the epicenter, while the latter could be stimulated by the acoustic-gravity waves from the partial transformation of the acoustic waves.

1. Introduction

Since the second half of the 20th century, more and more scientists have discovered that the earthquake preparation process manifests itself not only in the lithosphere, but also in the ionosphere. It is the first reports that the ionospheric disturbances associated with the earthquake were observed during the 1964 great Alaska earthquake [1,2]. Not long after that, Weaver et al. [3] also observed anomalous ionospheric disturbances following 1969 Kurile Islands earthquake. By analyzing the observations of ionospheric vertical sounding instrument, Antsilevich [4] and Datchenko et al. [5] found that the electron density increased over the epicenter before the 1966 Tashkent earthquake. Moreover, they thought the electron density abnormal increase may be the precursor of Tashkent earthquake. Hereafter, the ionospheric disturbances related to seismic activity, especially pre-earthquake ionospheric anomalies, aroused wide concern [6–16].

From the phenomena of ionospheric precursors to the reveal of the seismic-ionospheric coupling mechanism, the research on seismic-ionospheric effects has been conducted for more than 50 years. At present, it mainly focuses on the following two aspects: (1) detection and analysis of seismic-ionospheric precursors; (2) exploration of lithospheric (seismic)–atmospheric–ionospheric (LAI) coupling mechanism. On the first aspect mentioned above, Pulinets and Boyarchuk [17] pointed out that the minimum magnitude of earthquake which can disturb the ionosphere is *M*5,

* *Corresponding author.* Institute of Seismology, China Earthquake Administration, Wuhan, 430071, China.

E-mail address: 869244449@qq.com (Y. Zhou).

Peer review under responsibility of Institute of Seismology, China Earthquake Administration.

Production and Hosting by Elsevier on behalf of KeAi

http://dx.doi.org/10.1016/j.geog.2017.04.004

and the positive or negative seismic-ionospheric anomalies generally appear within one week before the earthquake. On the other hand, the explanation of the seismic-ionospheric coupling mechanism falls into the two main categories. One kind of explanation is that the vertical ground displacement or underground gas release caused by earthquake preparation excites the atmospheric acoustic-gravity waves, which propagate to the ionosphere and lead to the disturbances of electrons and ions [18–22]. The other kind of explanation is that earthquake fault rupture stimulates the formation of an additional vertical electric field, which penetrated into the ionosphere and caused a redistribution of charged particles [17,23–34].

Seismic-ionospheric precursor throws light on impending earthquake prediction, which is different from long-term prediction and has more significant benefits in reducing life casualties and property losses. Therefore, the pre-earthquake ionospheric anomalies were widely paid attention to in the academia. Recently, the studies on CIDs following strong earthquake have also been attached importance to by some scholars [35–41].

The nature of CIDs is that the vertical ground displacement caused by strong earthquake (focal zone dislocation and far-field Rayleigh wave) produces infrasonic pressure waves in the near-Earth atmosphere and excites acoustic-gravity waves which propagate into the ionosphere, where the coupling between neutral and ionized atmosphere results in the fluctuations of the ionospheric electron density. Since the atmospheric density decreases almost exponentially with altitude, energy conservation implies that the pulse amplitude increases upward as the sound waves propagates into the atmosphere. The amplification factor could reach 10^4 at ionospheric height [35], which makes it possible to detect the signals of seismic waves in the ionosphere.

The CID was observed mainly by the high-frequency Doppler sounding technique in the early stages, so it was not feasible to study the propagation of CID in detail because of a limited number of Doppler sounding stations. With the advent of GPS, not only the coseismic vertical ground displacement but also the ionospheric disturbances triggered by this displacement can be captured by a network of ground-based GPS receivers. GPS TEC technology was firstly used to study the CID by Calais and Minster [35]. They detected the near-field ionospheric TEC disturbances related to the 1994 Northridge earthquake in Southern California. Afraimovich et al. [37] also detected the ionospheric disturbances following two earthquakes in Turkey with GPS TEC technology. Since then, the GPS TEC technology becomes the most popular means of observing CID [42–47].

The ground-based GPS observation makes low-cost, high-precision and continuous ionospheric observations possible. This ionospheric observation technology can acquire the slant TEC which is an integral of electron density along the ray path between the GPS satellite and the receiver. Further, the TEC can be converted to the VTEC over the corresponding location. As for the calculation of VTEC, the reader may refer to the related papers [48–50]. Moreover, the two-dimensional VTEC distribution can be created in the observation area of ground-based GPS network, which makes it possible to determine the location and size of ionospheric anomalies [51].

In this paper, using GPS observations from the Crustal Movement Observation Network of China (CMONOC), we detect and analyze the ionospheric VTEC variations (in unit of TECu, 1 TECu = 10^{16} electrons/m^2) before and following the *M*7.8 Nepal earthquake which occurred at 06:11 UT on April 25, 2015 (https://www.usgs.gov). Fig. 1 demonstrates the distribution of GPS stations and the epicenter (28.2°E,84.7°E) of Nepal earthquake.

2. Detection and analysis of ionospheric anomalies before the *M*7.8 Nepal earthquake

In general, the day-to-day variation of VTEC over a fixed location will be small if the solar and geomagnetic activities keep relatively quiet in a period of time, which provides a reference background for detecting the ionospheric anomalies. For a time series of VTEC observations, the ionospheric anomalies are extracted by using sliding mean method. The method is depicted as follows.

To detect whether the ionospheric anomalies appear on a specified day, the VTEC observations within 10 days before the

Fig. 1. The distribution of GPS stations (green stars) and the epicenter (red star).

specified one is used as a background window (the VTEC observations affected by solar flares or magnetic storms should not be included in this background window. Otherwise, the affected VTEC observations will be replaced by the observations in the day before the background window). The VTEC observations over a fixed location at the same moment in the 10 days are extracted as a time series, which is assumed to follow a normal distribution with mean μ and standard deviation σ, then the anomalies are judged by examining whether the VTEC observation value on the specified day falls within the confidence interval $[\mu - 2\sigma, \mu + 2\sigma]$. If the examined VTEC observation is beyond the confidence interval, we thought that the ionospheric positive anomaly $(\Delta VTEC = VTEC - (\mu + 2\sigma) > 0)$ or negative anomaly $(\Delta VTEC = VTEC - (\mu - 2\sigma) < 0)$ occurs at the moment. Further, if large-scale VTEC anomalies appeared in the observation area and persisted for more than two hours, we would declare that the ionospheric anomalies happened on the specified day.

Considering the timeliness of short-impending earthquake prediction, we only examine whether there are the ionospheric anomalies within 20 days before the earthquake. This is mainly because a too long examining period is not conducive to reveal the correlation between seismic activity and ionospheric anomalies, and is not valuable practically in predicting the impending earthquake. In addition, the length of background window is set to 10 days, which is mainly because a too long background window is not suitable to describe the variation characteristics of current ionospheric state. Moreover, the adoption of sliding background window can ensure the authenticity and reliability of the detection result.

In order to have a visual display of ionospheric anomalies, the detection of pre-earthquake ionospheric anomalies is carried out for the two-dimensional time-series VTEC distribution in China and its adjacent regions. The detection result shows that the positive ionospheric anomalies appeared from 12:00 UT to 16:00 UT on April 23. Fig. 2 illustrates the distribution of the ionospheric anomalies (ΔVTEC) at 14:00 UT on April 23. Seen from Fig. 2, the ionospheric anomalies located in east–south of the epicenter and covered a long and narrow area which has almost a spatial scale of thousands of kilometers. Moreover, relative to the non-perturbed state of the ionosphere, the maximum variability amplitude of the ionospheric VTEC around the epicenter exceeds 70% at the peak of the ionospheric anomalies (Fig. 3).

However, are the ionospheric anomalies associated with the *M*7.8 Nepal earthquake? Taking the significant effects caused by solar and geomagnetic activities on the ionosphere into consideration, we investigated the solar radio flux F10.7, geomagnetic indices Kp and Dst. Seen from Fig. 4, the solar-terrestrial environment was relatively quiet after April 21, so the ionospheric anomalies on April 23 couldn't come from the sudden variation of the solar or geomagnetic activity. Moreover, the ionospheric anomalies have a local effect. In addition, due to the thermospheric dynamics caused by various types of atmospheric disturbances from lower atmosphere, the ionosphere may generate significant day-to-day variations. However, compared with a non-perturbed state of the ionosphere, the relative variability associated with thermospheric dynamics usually does not go beyond 30% [52–54]. Further, using the GIM provided by CODE, we also detected the ionospheric anomalies over China. Moreover, a magnetically conjugated effect in the ionosphere was observed in the southern hemisphere (Fig. 5). However, the amplitude and space size of ionospheric anomalies in the magnetically conjugated region are smaller than those near the epicenter. The conjugated phenomena of pre-earthquake ionospheric anomalies were also reported [9,11,17,55,56]. Generally speaking, the relatively quiet solar-terrestrial environment could not cause large ionospheric disturbances. Therefore, the positive anomalies on April 23 could be related to *M*7.8 Nepal earthquake.

3. The CID following *M*7.8 Nepal earthquake

The detection object of pre-earthquake ionospheric anomalies is the VTEC, while the detection object of CID is the slant TEC along the line-of-sight (LOS) from the receiver to the GPS satellite in this paper. The TEC variation mainly reflects the electron density changes near the ionospheric pierce point (IPP) which is the intersection of the LOS and a single layer (it is assumed that all the electrons are concentrated in an infinitely-thin layer at the altitude of about 350 km above the Earth's surface). In a continuous process of observing a GPS satellite with a ground-based receiver, if the ionosphere is under quiet ionospheric condition, the TECs derived from dual-frequency observations should have a good continuity and could not have sudden disturbances in this process. Therefore, the quiet space environment makes the detection of ionospheric disturbances possible in a short period of time.

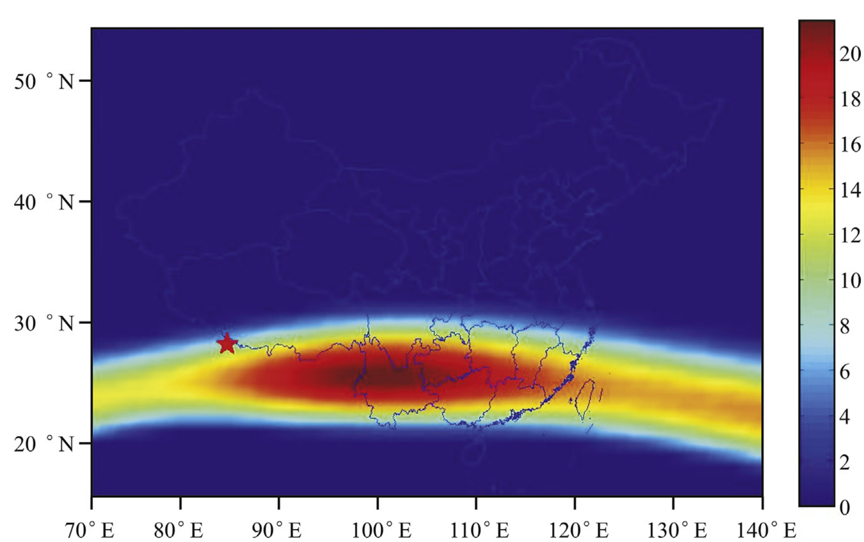

Fig. 2. The distribution of the ionospheric anomalies (unit: TECu) over the epicenter of Nepal earthquake at 14:00 UT on April 23, 2015. The red star indicates the epicenter.

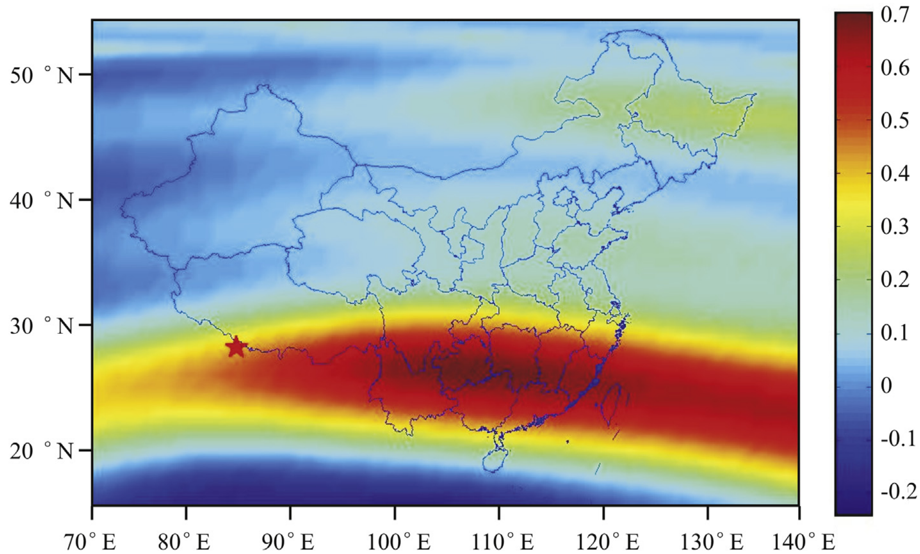

Fig. 3. In comparison with the mean value of the previous 10 days' data, the distribution of the relative variability (unit: 100%) of the VTEC around the epicenter of Nepal earthquake at 14:00 UT on April 23, 2015. The red star indicates the epicenter.

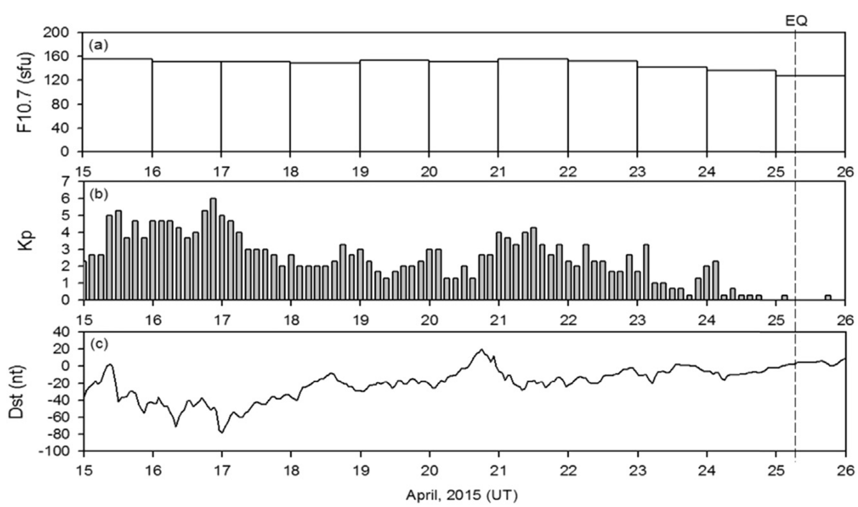

Fig. 4. The indices of solar and geomagnetic activities from April 15 to April 26, 2015. (a) The 10.7 cm solar radio flux, F10.7; (b) the global geomagnetic Kp index; (c) the geomagnetic equatorial Dst index. The vertical dashed line indicates the occurrence time of Nepal earthquake.

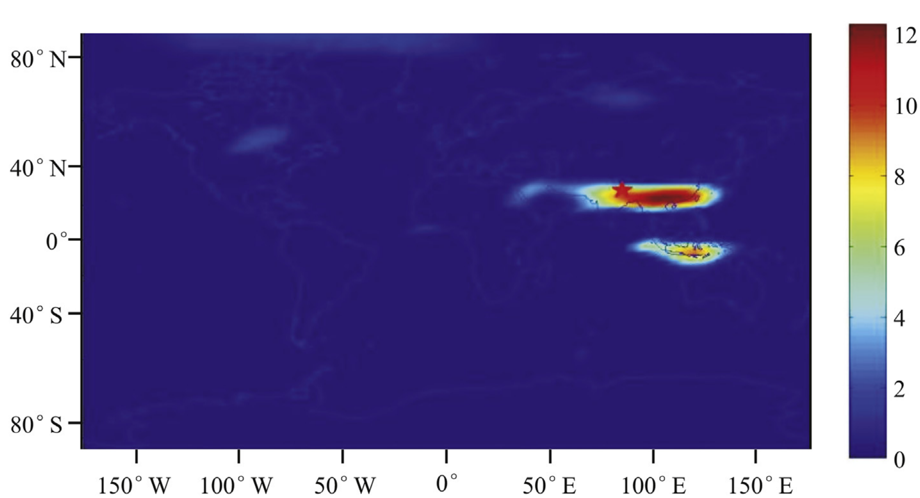

Fig. 5. The distribution of the global ionospheric anomalies (unit: TECu) from CODE GIM at 14:00 UT on April 23, 2015. The red star indicates the epicenter.

In this paper, the detection method of CID is as follows. (1) A time series of TECs is constructed in a specified period of time, and one hour immediately after the earthquake is assumed to be the detection period of ionospheric disturbances. (2) The TEC data within one hour before and after the detection period were selected to set up a normal ionospheric background, namely, a 6-order polynomial which was used to fit the two-hour TEC data with least-squares solution. (3) The time series of the residuals from the observed TEC minus the fitted TEC with the 6-order polynomial used as the high-pass filter in the detection period corresponds to the ionospheric disturbances, and the larger residuals correspond to the CIDs. Accordingly, based on the distances among the IPPs of the maximum disturbances at different station-satellite pairs and the corresponding time delays, the propagation speed of CID excited by earthquake in the ionosphere can be roughly estimated.

The CID following the Nepal earthquake was detected by using 13 high-frequency (1 Hz) GPS stations from CMONOC. Fig. 6 shows the distribution of 13 stations and the projections of the IPP trajectories on the ground. The detection results show that ionospheric TEC disturbances with an amplitude of 0.5 TECu were firstly observed at the stations nearer to the epicenter about 12 min after the earthquake. With the passage of time, the more distant stations also observed the ionospheric disturbances in succession (Fig. 7).

Further, more detailed information about the evolution of the disturbances can be obtained from a travel time diagram of CID. By analyzing the arrival time and distance of the maximum CIDs at different station-satellite pairs, the propagation speed of ionospheric disturbances can be estimated. As can be seen from Fig. 8, the CID triggered by the Nepal earthquake exhibits two propagation speeds, namely 877 $\pm$ 75 m/s and 319 $\pm$ 30 m/s, which correspond to the propagation speeds of acoustic waves and acoustic-gravity waves at the ionospheric height, respectively. At a distance of about 450 km from the epicenter, the CID amplitude caused by the former reached the maximum value of 0.5 TECu, and then decreased in the far field. Immediately following the former, the latter triggered a relatively little CID with the maximum amplitude of 0.2 TECu. Fig. 9 describes the simulated sound velocity based on linear-acoustic ray theory in the atmosphere and ionosphere. It is not hard to see, the estimated speed of acoustic waves is almost consistent with that of simulated calculation. Unfortunately, in our analysis of the CID, the ionospheric disturbances triggered by the earthquake Rayleigh surface waves failed to be clearly detected.

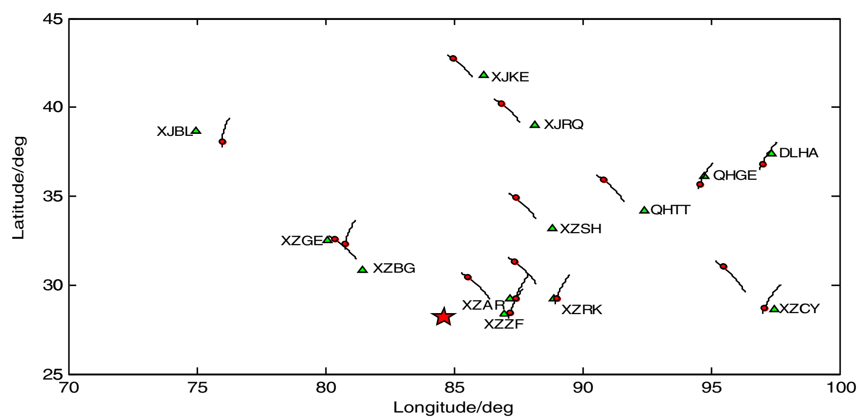

Fig. 6. The distribution of high-frequency GPS stations (green stars) and IPP trajectories (black thin curves) during 06:00–07:00 UT on April 25, 2015. The red star indicates the epicenter. The little red dots on the trajectories indicate the locations of IPPs at the occurrence time of Nepal earthquake.

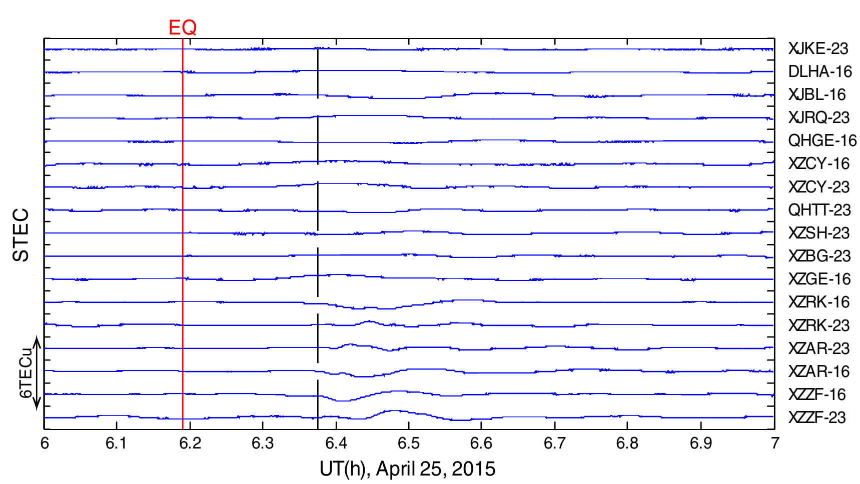

Fig. 7. The TEC residual time series of 17 station-satellite pairs before and after Nepal earthquake. The red line indicates the occurrence time of Nepal earthquake. The black dashed line indicates the time when the CID has been firstly observed by the nearest GPS station.

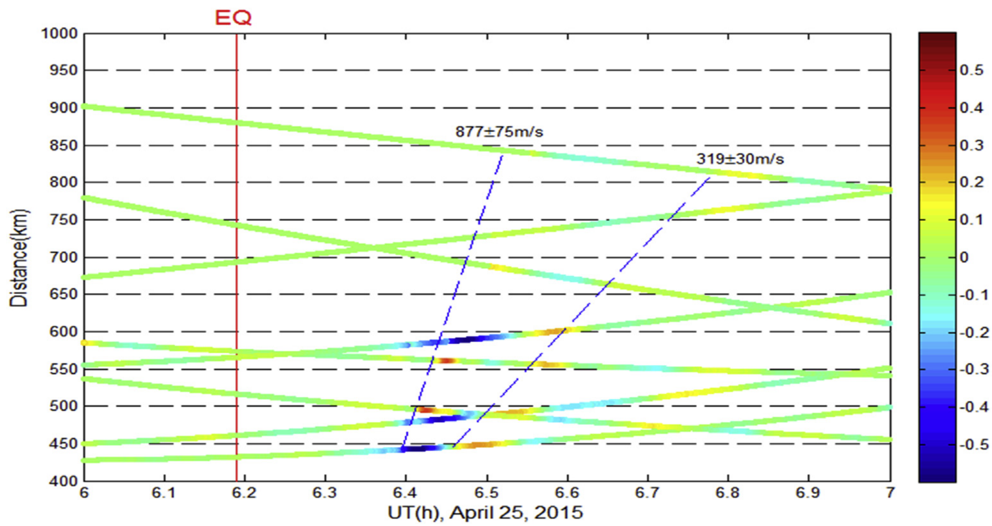

Fig. 8. The TEC residual time series (unit: TECu) with the time and distance. The red line indicates the occurrence time of Nepal earthquake. The blue dashed lines indicate the propagation speeds of CID after Nepal earthquake occurrence.

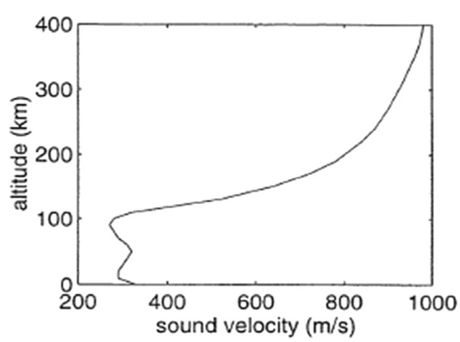

Fig. 9. The simulated sound velocity in the atmosphere and ionosphere [57].

4. Discussion and conclusion

Analyzing the ground-based GPS VTEC data, we found the positive ionospheric anomalies two days before the 2015 *M*7.8 Nepal earthquake. The spatial sizes of the pre-earthquake ionospheric VTEC enhancement by more than 30% were larger than 1000 km in latitude and 4000 km in longitude. Moreover, the ionospheric anomalies lasted about 4 h. In view of the solar-terrestrial environment and the characters of the ionospheric anomalies, we think that the remarkable increase of VTEC around the epicenter on April 23 could be the ionospheric precursors of Nepal earthquake. In addition, we also detected the CIDs following this earthquake and identified the two propagation speeds of ionospheric disturbances which correspond to the effects of acoustic waves and acoustic-gravity waves, respectively. The former triggered a larger ionospheric disturbance than the latter.

As mentioned in the introduction, two kinds of seismic-ionospheric mechanisms are developed to explain the phenomena of pre-earthquake ionospheric anomalies. The acoustic-gravity wave mechanism was once very popular, but Pulinets and Boyarchuk [17] held a negative attitude to this mechanism. They thought that this mechanism could not be verified in practice, since the ionospheric disturbances simulated by acoustic-gravity waves are very small. Using GPS TEC data for the first time, Calais and Minster [35] detected and analyzed ionospheric disturbances after the *M*w6.7 Northridge earthquake in the January 1994. They found that the TEC disturbances following the Northridge earthquake are lower 2–2.5 orders of magnitude than the normal ionospheric background, which was also confirmed by theoretical calculations [36]. Ionospheric disturbances caused by acoustic-gravity waves are so small that it will be drowned in relatively larger day-to-day ionospheric variations, so it is almost impossible to detect such weak seismic-ionospheric precursors [17]. As far as the Nepal earthquake discussed above, the amplitude of pre-earthquake ionospheric anomalies was much larger than that of CID.

At the same time, the additional vertical electric field mechanism for seismic-ionospheric coupling has been put forward. How is this electric field generated in seismogenic zone? Some opinions have been proposed for the generation of this electric field, such as the electric field effect of geochemical process [17,58], the piezoelectric potential effect of rock [24–27], the flow potential effects of groundwater [59], and the friction electromagnetic effects [28]. Among these opinions, the first two gained more attention. Despite all that, there is still no consensus on the seismic-ionospheric coupling mechanism. Therefore, a further study on the coupling mechanism is needed, which helps to clarify and reveal the truth of pre-earthquake ionospheric anomalies.

Up to now, the large-scale continuously operating reference station (CORS) network allowed us to observe the CID and track its evolution, which may provide us more information about the process of a wave transformation from the ground to the ionosphere. CID can be observed both near the epicenter and far from it. However, the physical mechanisms of their generation are different, so their parameters (e.g., velocity of CID propagation, period, and duration) differ markedly. The source of such CID can be the main quake itself (e.g., the vertical ground displacement or soil gas release around the epicenter), seismic surface Rayleigh waves, etc.

Seismometers have long been used to locate earthquake hypocenters and get the tomographic images of the lithosphere and upper mantle based on the inversion of surface wave group or phase velocities. However, the above research works are strongly dependent on the distribution and number of seismometers. Based on thousands of permanent ground-based GPS receivers, they can provide an indirect measurement of the local group velocity of Rayleigh waves in space and time. Therefore, the observation of CID from Rayleigh surface waves will complement the data produced by seismic network. A combination of the GPS TEC observation and standard seismological techniques, the ray-tracing and beam-forming searches, can be used to accurately locate the origin and estimate the propagation velocity of CID triggered by a strong earthquake [60]. So, the CID monitoring has a practical significance in determining the hypocenter parameters, understanding the crustal structure, and assisting the tsunami warning [61].

Acknowledgements

The authors thank the CMONOC, CODE, and NOAA/NCEI for providing GPS observations, the global ionosphere map data, and the solar and geomagnetic field data, respectively. This work is supported by National Natural Science Foundation of China (41174030, 41304047).

References

[1] R.S. Leonard, R.A. Barnes, Observations of ionospheric disturbances following the Alaska earthquake, J. Geophys. Res. 70 (5) (1965) 1250–1253.
[2] K. Davies, D.M. Baker, Ionospheric effects observed around the time of the Alaskan earthquake of March 28, 1964, J. Geophys. Res. 70 (9) (1965) 2251–2253.
[3] P.F. Weaver, P.C. Yuen, G.W. Prolss, A.S. Furumoto, Acoustic coupling into the ionosphere from seismic waves of the earthquake at Kurile Island on August 11, 1969, Nature (226) (1970) 1239–1241.
[4] M.G. Antsilevich, The influence of Tashkent earthquake on the Earth's magnetic field and the ionosphere, Tashkent earthquake 26 April 1966, Tashkent. FAN Publ. (1971) 187–188.
[5] E.A. Datchenko, V.I. Ulomov, C.P. Chernyshova, Electron density anomalies as the possible precursor of Tashkent earthquake, Dokl. Uzbek. Acad. Sci. 12 (1972) 30–32.
[6] Yongsheng Li, Kaichun Li, Ionospheric disturbances during large earthquakes, Acta Seismol. Sin. 9 (1) (1987) 101–107 (in Chinese).
[7] Pinren Du, Herong Jiang, Jianshan Guo, Research on possibility of ionospheric anomalies as an earthquake precursor, Earthquake 18 (2) (1998) 119–126 (in Chinese).
[8] J.Y. Liu, Y.J. Chuo, S.J. Shan, Y.B. Tsai, Y.I. Chen, S.A. Pulinets, et al., Pre-earthquake ionospheric anomalies registered by continuous GPS TEC measurements, Ann. Geophys. 22 (5) (2004) 1585–1593.
[9] B. Zhao, M. Wang, T. Yu, W.X. Wan, J.H. Lei, L.B. Liu, et al., Is an unusual large enhancement of ionospheric electron density linked with the 2008 great Wenchuan earthquake, Geophys. Res. Lett. (2008) 113, http://dx.doi.org/10.1029/2008JA013613 (A11).
[10] Y. He, D. Yang, J. Qian, M. Parrot, Response of the ionospheric electron density to different types of seismic events, Nat. Hazards Earth Syst. Sci. 11 (8) (2011) 2173–2180.
[11] Y.B. Yao, P. Chen, S. Zhang, J.J. Chen, F. Yan, W.F. Peng, Analysis of pre-earthquake ionospheric anomalies before the global M = 7.0+ earthquakes in 2010, Nat. Hazards Earth Syst. Sci. 12 (3) (2012) 575–585.
[12] K. Heki, Y. Enomoto, Preseismic ionospheric electron enhancements revisited, J. Geophys. Res. 118 (10) (2013) 6618–6626.
[13] Y.Y. Ho, H.K. Jhuang, Y.C. Su, J.Y. Liu, Seismo-ionospheric anomalies in total electron content of the GIM and electron density of DEMETER before the 27 February 2010 M8.8 Chile earthquake, Adv. Space Res. 51 (12) (2013) 2309–2315.
[14] X. Zhang, C. Fidani, J. Huang, J. Qian, Burst increases of precipitating electrons recorded by the DEMETER satellite before strong earthquakes, Nat. Hazards Earth Syst. Sci. 13 (1) (2013) 197–209.
[15] F.Y. Zhu, Y.Y. Zhou, J. Lin, F.F. Su, A statistical study on the temporal distribution of ionospheric TEC anomalies prior to M7.0+ earthquakes during 2003–2012, Astrophys. Space Sci. 350 (2) (2014) 449–457.
[16] H. Le, J. Liu, B. Zhao, L. Liu, Recent progress in ionospheric earthquake precursor study in China: a brief review, J. Asian Earth Sci. 114 (2015) 420–430.
[17] S.A. Pulinets, K. Boyarchuk, Ionospheric Precursors of Earthquakes, Springer, Heidelberg, Berlin, 2004.
[18] S.V. Garmash, Y.M. Lin'kov, L.N. Petrova, G.M. Shved, Generation of atmospheric oscillations by seismic-gravity oscillations of the Earth, Izvest. Atmos. Ocean Phys. 25 (1989) 952–959.
[19] G.I. Voitov, I.P. Dobrovolsky, Chemical and isotopic-carbon instabilities of the native gas flows in seismically active regions, Izvest. Earth Sci. 3 (1994) 20–31.
[20] V.V. Hegai, V.P. Kim, L.I. Nikiforova, A possible generation mechanism of acoustic-gravity waves in the ionosphere before strong earthquakes, J. Earthq. Predict. Res. 6 (1997) 584–589.
[21] S.L. Shalimov, M.B. Gokhberg, Lithosphere–ionosphere coupling mechanism and its application to the earthquake in Iran on June 20, 1990. A review of ionospheric measurements and basic assumptions, Phys. Earth Planet. Interr. 105 (1998) 211–218.
[22] E.A. Mareev, D.I. Ludin, O.A. Molchanov, Mosaic source of internal gravity waves associated with seismic acvity, in: M. Hayakawa, O.A. Molchanov (Eds.), Lithospheric–Atmospheric–Ionospheric coupling, Terra SciPubl, Tokyo, 2002, pp. 335–342.
[23] J. Hao, The anomalous of atmospheric electric field at the ground level and earthquakes, Acta Seismol. Sin. 10 (2) (1988) 207–212.
[24] F. Freund, Lee J. WhangE, Highly mobile charge carriers in minerals, in: M. Hayakawa, Y. Fujinawa (Eds.), Electromagnetic Phenomena Related to Earthquake Prediction, Terra Sci. Publ. Chem, Tokyo, 1994, pp. 271–277.
[25] V. Hadjicontis, C. Mavromatou, Electric signals recorded during uniaxial compression of rock samples: their possible correlation with pre-seismic electric signals, Acta Geophys. Pol. 43 (1995) 49–61.
[26] F. Freund, Time-resolved study of charge generation and propagation in igneous rocks, J. Geophys. Res. 105 (B5) (2000) 11001–11019.
[27] R. Teisseyre, Dislocation dynamics and related electromagnetic excitation, Acta Geophys. Pol. 49 (2001) 55–73.
[28] A. Takeuchi, H. Nagahama, T. hashimoto, Surface electrification of rocks and charge trapping centers, Phys. Chem. Earth Parts A/B/C 29 (4–9) (2004) 359–366.
[29] S. Yoshida, T. Ogawa, Electromagnetic emissions from dry and wet granite associated with acoustic emission, J. Geophys. Res. 109 (B9) (2004), http://dx.doi.org/10.1029/2004JB003092.
[30] A.A. Namgaladze, M.V. Klimenko, V.V. Klimenko, I.E. Zakharenkova, Physical mechanism and mathematical modeling of earthquake ionospheric precursors registered in total electron content, Geomagnetism Aeronomy 49 (2) (2009) 252–262.
[31] R.G. Harrison, K.L. Aplin, M.J. Rycroft, Atmospheric electricity coupling between earthquake regions and the ionosphere, J. Atmos. Sol. Terr. Phys. 72 (5–6) (2010) 376–381.
[32] S.A. Pulinets, D. Davidenko, Ionospheric precursors of earthquakes and global electric circuit, Adv. Space Res. 53 (5) (2014) 709–723.
[33] K. Ryu, E. Lee, J.S. Chae, M. Parrot, S.A. Pulinets, Seismo-ionospheric coupling appearing as equatorial electron density enhancements observed via DEMETER electron density measurements, J. Geophys. Res. 119 (10) (2014) 8524–8542.
[34] X. Zhang, X. Shen, S. Zhao, L. Yao, X. Ouyang, J. Qian, The characteristics of quasi-static electric field perturbations observed by DEMETER satellite before large earthquakes, J. Asian Earth Sci. 79 (2014) 42–52.
[35] E. Calais, J.B. Minster, GPS detection of ionospheric TEC perturbations following the January 17, 1994, Northridge Earthq. Geophys. Res. Lett. 22 (9) (1995) 1045–1048.
[36] J.B. Davies, C.B. Archambeau, Modeling of atmospheric and ionospheric disturbances from shallow seismic sources, Phys. Earth Planet. Interr. 105 (1998) 183–199.
[37] E.L. Afraimovich, N.P. Perevalova, A.V. Plotnikov, A.M. Uralov, The shock-acoustic waves generated by the earthquakes, Ann. Geophys. 19 (4) (2001) 395–409.
[38] K. Heki, J.S. Ping, Directivity and apparent velocity of the coseismic ionospheric disturbances observed with a dense GPS array, Earth Planet. Sci. Lett. 236 (2005) 845–855.
[39] E. Astafyeva, K. Heki, Dependence of waveform of near-field coseismic ionospheric disturbances on focal mechanisms, Earth Planets Space 61 (2009) 939–943.
[40] T. Tsugawa, A. Saito, Y. Ostuka, M. Nishioka, T. Maruyama, H. Kato, et al., Ionospheric disturbances detected by GPS total electron content observation after the 2011 off the Pacific coast of Tohoku earthquake, Earth Planets Space 63 (2011) 875–879.
[41] M.N. Cahyadi, K. Heki, Ionospheric disturbances of the 2007 Bengkulu and the 2005 Nias earthquakes, Sumatra, observed with a regional GPS network, J. Geophys. Res. 118 (4) (2013) 1777–1787, http://dx.doi.org/10.1002/jgra.50208.
[42] V. Ducic, J. Artu, P. Lognonné, Ionospheric remote sensing of the Denali earthquake Rayleigh surface waves, Geophys. Res. Lett. 30 (18) (2003) 1801–1804.
[43] Y. Otsuka, N. Kotake, T. Tsugawa, K. Shiokawa, T. Ogawa, Effendy, et al., GPS detection of total electron content variations over Indonesia and Thailand following the 26 December 2004 earthquake, Earth Planet Space 58 (2) (2006) 159–165.
[44] E.L. Afraimovich, F. Ding, V.V. Kiryushkin, E.I. Astafyeva, Near-field TEC response to the main shock of the 2008 Wenchuan earthquake, Earth Planet Space 62 (11) (2010) 899–904.
[45] G. Occhipinti, L. Rolland, P. Lognonne, S. Watada, From Sumatra 2004 to Tohoku-Oki 2011: the systematic GPS detection of the ionospheric signature induced by Tsunamigenic earthquakes, J. Geophys. Res. 118 (6) (2013) 3626–3636.
[46] E. Astafyeva, L. Rolland, A. Sladen, Strike-slip earthquakes can also be detected in the ionosphere, Earth Planet Sci. Lett. 405 (2014) 180–193.
[47] Peng Chen, Yibin Yao, Jiajun Chen, Wanqiang Yao, Xuejun Zhu, Study of the 2013 Lushan M7.0 earthquake coseismic ionospheric disturbances, Adv. Space Res. 54 (11) (2014) 2194–2199.
[48] E. Sardon, A. Rius, N. Zarraoa, Estimation of the transmitter and receiver differential biases and the ionospheric total electron content from global positioning system observations, Radio Sci. 29 (3) (1994) 577–586.
[49] A.J. Manucci, B.D. Wilson, D.N. Yuan, C.H. Ho, U.J. Lindqwister, T.F. Runge, A global mapping technique for GPS-derived ionospheric total electron content measurements, Radio Sci. 33 (3) (1998) 565–582.
[50] S. Schaer, Mapping and Predicting the Earth's Ionosphere using the Global Positioning System (Dissertation of Doctoral Degree), University of Berne, Berne, 1999.

[51] Yiyan Zhou, Yun Wu, Xuejun Qiao, Xunxie Zhang, Ionospheric anomalies detected by ground-based GPS before the Mw7.9 Wenchuan earthquake of May 12, 2008, China J. Atmos. Sol. Terr. Phys. 71 (8–9) (2009) 959–966.
[52] J.M. Forbes, S.E. Palo, X. Zhang, Variability of the ionosphere, J. Atmos. Sol. Terr. Phys. 62 (8) (2000) 685–693.
[53] H. Rishbeth, M. Mendillo, Patterns of F2-layer variability, J. Atmos. Sol. Terr. Phys. 63 (15) (2001) 1661–1680.
[54] M. Mendillo, H. Rishbeth, R.G. Roble, J. Wroten, Modelling F2-layer seasonal trends and day-to-day variability driven by coupling with the lower atmosphere, J. Atmos. Sol. Terr. Phys. 64 (18) (2002) 1911–1931.
[55] S.A. Pulinets, V.A. Alekseev, A.D. Legenka, V.V. Hegai, Radon and metallic aerosols emanation before strong earthquakes and their role in atmosphere and ionosphere modification, Adv. Space Res. 20 (11) (1997) 2173–2176.
[56] J.Y. Liu, H. Le, Y.I. Chen, C.H. Chen, L. Liu, W. Wan, et al., Observations and simulations of seismoionospheric GPS total electron content anomalies before the 12 January 2010 M7 Haiti earthquake, J. Geophys. Res. 116 (A4) (2011), http://dx.doi.org/10.1029/2010JA015704.
[57] E. Calais, J.B. Minster, M.A. Hofton, M.A.H. Hedlin, Ionospheric signature of surface mine blasts from global positioning system measurements, Geophys. J. Int. 132 (1) (1998) 191–202.
[58] E.P. Krider, R.W. Roble, The Earth's Electrical Environment, National Academy Press, Washing DC, 1986.
[59] V.V. Kormiltsev, A.N. Ratuchnyak, V.A. Shapiro, Three-dimensional modeling of electric and magnetic fields induced by the fluid flow movement in porous media, Phys. Planet. Inter 105 (3–4) (1998) 109–118.
[60] J.Y. Liu, H.F. Tsai, C.H. Lin, M. Kamogawa, Y.I. Chen, C.H. Lin, et al., Coseismic ionospheric disturbances triggered by the Chi-Chi earthquake, J. Geophys. Res. 115 (A8) (2010), http://dx.doi.org/10.1029/2009JA014943.
[61] Tang long, Research on Travelling Ionospheric Disturbances Detection and Application in Tsunami Monitoring using GPS (PhD Dissertation), Wuhan University, 2015 (in Chinese).

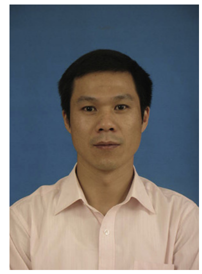

Yiyan Zhou, an associate professor from the Institute of Seismology, China Earthquake Administration. He is mainly engaged in the research on the seismo-ionospheric effects.